Catalysis Today 177 (2011) 39–49

Contents lists available at ScienceDirect

Catalysis Today

journal homepage: www.elsevier.com/locate/cattod

Synergy between iono-covalent bonds and van der Waals interactions in SAMs formation: A first-principles study of adsorption of carboxylic acids on the Zn–ZnO(0 0 0 1) surface

M.M. Islam[1], B. Diawara*, P. Marcus, D. Costa*

Laboratoire de Physico-Chimie des Surfaces, UMR CNRS-ENSCP 7045, Ecole Nationale Supérieure de Chimie de Paris, Chimie-Paristech, 11 rue P. et M. Curie, 75005, Paris, France

ARTICLE INFO

Article history:
Received 9 February 2011
Received in revised form 1 June 2011
Accepted 6 June 2011
Available online 27 July 2011

Keywords:
DFT
Carboxylic acid
ZnO
Green coating
Dispersion correction
van der Waals
Self-assembled monolayers
Acid–base reaction
Inner sphere adsorption

ABSTRACT

The adsorption of carboxylic acids (CA) on the Zn–ZnO(0 0 0 1) surface was studied by density functional theory including dispersion forces (DFT + D) calculations. Carboxylic acids of formula $CH_3(CH_2)_{n-2}COOH$ (where $n = 1–10$ is the total number of C atoms in the CA) were considered. In a first step, the formation of the iono-covalent bonds with the surface was studied with standard DFT approach, while the self-assembling properties were examined through dispersion corrected DFT-D approach. Comparing different possible adsorption modes, it is concluded that the most likely mechanism for CA adsorption on the Zn–ZnO(0 0 0 1) surface is dissociative bridging adsorption with the carboxylate group attached to two Zn atoms and the proton transferred to the neighbouring Zn atom, forming a Zn–H bond. The effect of the chain length was investigated. The energy of formation of the iono-covalent bond decreases from the formic acid (−1.62 eV) to the propionic acid (−2.11 eV) and then reaches a plateau. In a second part, the orientation of the molecule to the surface and the energy of adsorption including van der Waals contributions were investigated. The adsorption energy decreases with increasing chain length (to reach the value of −2.77 eV for $n = 9$), thanks to the stabilization through bending of the molecules to the surface and lateral van der Waals interactions. The tilt angle to the surface is 35°. A transition from perpendicular to tilted structures is calculated for $n = 7$. The interaction of the CA with the surface was analyzed by means of electronic core level shifts and PDOS analysis.

1. Introduction

Organic coatings are widely used industrially to protect metal and alloy surfaces from corrosion [1–4]. The adhesion of the organic molecules and coatings with metallic or oxide surfaces has been an important issue for many years in corrosion science [5,6]. Organic compounds containing polar group including nitrogen, sulfur, oxygen atoms and heterocyclic compounds with polar functional groups and conjugated double bonds have been reported as corrosion inhibitors. The inhibitory activity of these organic compounds is usually attributed to their interactions with the metal/alloy surface via their adsorption. Polar functional group is considered as the reaction centre that stabilizes the adsorption process.

Since a few years, the concept of "green coatings" has been developed, as environmental friendly technologies are increasingly required for surface treatments. Among others, two families of compounds are possible candidates for the "green coating" alternatives: carboxylic acids and amines. Carboxylic acids are promising molecules for their non-toxicity, adhesion characteristics and protective character, to be used in substitution to chromate conversion layers. Aliphatic carboxylic acids of different chain lengths have been shown to inhibit the corrosion of iron, lauric acid being the most efficient among the acids studied [7]. Propionic acid was used for corrosion protection of iron [8], lauric acid has protective properties for mild steel in neutral medium [9]. Formic, acetic, glutaric and butyric acids have also inhibition properties on Cu, formic acid being the most protective [10]. The inhibitor properties of dodecanoic acid on stainless steel in aqueous NaCl solution at pH 4 were also evidenced [11]. Polyglutamate and polyaspartate decrease the corrosion rates of Al alloys [12], due to a strong adhesion on alumina [13].

Carboxylic acid (CA) groups are capable of bonding with the oxide surface by "inner sphere adsorption" (see reviews [14,15] for the description of this concept), in substituting surface hydroxyl groups and forming coordinatively bonded carboxylate species

* Corresponding authors.
E-mail addresses: bob-diawara@chimie-paristech.fr (B. Diawara), dominique-costa@chimie-paristech.fr (D. Costa).
[1] Present address: Institut für Physikalische und Theoretische Chemie, Universität Bonn, Wegelerstrasse 12, 53115 Bonn, Germany.

0920-5861/$ – see front matter © 2011 Elsevier B.V. All rights reserved.
doi:10.1016/j.cattod.2011.06.007

[16], the adsorption occurring through an acid–base reaction leaving the conjugate base COO^- bonded to a Lewis acid at the surface. The adsorption mode of CA to surfaces was investigated through experimental [17–24] and theoretical studies [25–46]. Depending on the substrate, the binding mode may be of outer sphere type [26–29], or inner sphere non dissociative [43,44] or dissociative [19–24]. The dissociative adsorption may be unidentate [18], bidentate [17] or bridging [30,42,45,46].

However, in the theoretical studies, although the binding mode with the surface was carefully studied, very often CA self-assembly properties were not considered. In fact, the corrosion inhibitor properties of organic molecules with alkyl chains are linked with their capacity to self assemble at the surface in compact layers [47–49]. For example, *n*-alkaloic acids form self assembled monolayers (SAM) on Al_2O_3 [50–56] and docosanoic acid forms a $p(2 \times 2)$ overlayer structure on AgO, with a lattice spacing of 5.78 Å [57].

In recent years, SAM formation has attracted the interest of theoreticians, especially SAMs formed on metal surfaces [58–62]. It is well known that a strong interaction of the molecule's head with the surface as well as the capacity of self organization by stacking of the hydrophobic chains explain the singular capacity of those organic molecules to self assemble at surfaces [47,63]. Among other possible applications, their capacity to form dense ordered layers is responsible for their protective properties against corrosion of metals.

As other oxides, ZnO may interact with carboxylic acids. Especially, the (0 0 0 1)–Zn-terminated surface is more reactive towards carboxylic acids adsorption than the (0 0 0 1)–O-terminated one and the non-polar surfaces [64]. Carboxylic acids may also be efficient in atmospheric corrosion of Zn [65]. They are also used for ZnO nanoparticles functionalization [66].

In the present work we have studied the adsorption of carboxylic acids on the Zn-terminated ZnO(0 0 0 1) surface, for various chain lengths. ZnO has been chosen as it covers the surface of Zn and galvanized steels and thus of great interest for industrial applications. Indeed an inhibition layer may protect the oxide surface against adsorption of aggressive species.

We have explored the influence of the aliphatic chain length on the adsorption of CA. Indeed, one interesting question in experimental and theoretical studies is the validity of using a small molecule as a model to represent real inhibition layers. For example, formic or acetic acids are used in experiment study to model larger carboxylic acids [7]. This problem was handled in two steps: in the first part, we have examined the adsorption mode and energy of CA of increasing chain length on ZnO without lateral interactions, by means of a pure DFT approach. By this way, the specific role of the chain length on the adsorption mode and energy of formation of the iono-covalent bonds is investigated. The molecule–surface interaction is analyzed by means of electronic analysis calculations such as core level shifts and density of states. In the second part of this work, we take benefit from the recently implemented van der Waals forces in VASP package and examine the effect of lateral interactions on the adsorption energies and geometries as a function of the chain size. In particular, we explore the tilt angle of the CA molecules to the ZnO surface. Indeed, it is well known that SAMs, to optimize lateral interactions, may bend towards the surface: thiols on gold often bend by 26–28° to the normal to the surface [47]. More important tilt angles can be found in other systems, e.g. for alkanethiolates on AsGa (57° tilt) [67]. On oxides, the picture is not unique [47]: as an example, Tao found that fatty acids adsorb perpendicular to the Al_2O_3 surface [53]. Samart et al. [57] found that docosanoic acid monolayers on AgO are tilted 26°7′ from the surface normal. In contrast, other studies report that CA SAMs on AgO are normal to the surface [47]. The tilt angle is an important parameter to be studied as it is directly related to the wetting properties of the SAM.

2. Computational details

The periodic calculations were performed using the DFT method based on the GGA approximation employing the Perdew–Wang (PW91) exchange-correlation functional [68,69]. This method was used as implemented in the plane-wave program VASP [70,71]. The projector-augmented wave (PAW) potentials [72,73] were used for the core electron representation with a PAW core radius of 1.52 Å for oxygen. With plane wave methods, the quality of the basis set is determined by a single parameter, the energy cutoff E_{cut}. We used a converged value of E_{cut} = 400 eV, as in previous studies [42,74]. The integration in reciprocal space was performed with a Monkhorst–Pack grid [75]. The k-points grid was set to $8 \times 8 \times 8$ for the bulk cell, and the energy convergence was achieved at 10^{-4} eV/cell. For the (2×2) slabs, a K-POINT grid of $(4 \times 4 \times 1)$ was used.

ZnO crystallizes in the space group P63mc. In the bulk structure, all Zn and O arrangements are hexagonal with atoms occupying tetrahedral sites. The unit cell of the bulk ZnO contains 2 ZnO units. The optimized cell parameters are a = 3.25 Å and c = 5.24 Å, in good agreement with the experimental values (a = 3.2497 Å, c = 5.2042 Å) [76]. Based on the optimized structure of bulk ZnO, five Zn–O bilayer slabs of Zn terminated (0 0 0 1) surface were modeled for (2×2) supercells, as explained in Ref. [42]. A vacuum layer of 25 Å along the z direction perpendicular to the surface (x and y being parallel to the surface) was employed to prevent interactions between the repeated slabs. The chain length of studied CAs varies from 0 Å (for n = 1) to 13.50 Å (for n = 10) as given in Table 1. A dipolar correction was introduced along the z axis perpendicular to the surface to take into account the polarity of the surface and the molecule. The dipolar and quadripolar corrections were 0.02–0.03 eV/adsorbed molecule. The central and bottom layers in the slab were kept frozen in the geometry of the bulk, whereas the Zn–O–Zn surface

Table 1
Energies of adsorption of carboxylic acids of increasing sizes on the ZnO surface (coverage 2.6 CA/nm^2). The mode of adsorption is dissociative bridging. Numbers in parenthesis indicate the energy of adsorption in the unidentate mode, numbers in double parenthesis indicate the energy of adsorption in the bidentate mode.

n	Formula and name	Chain length (Å)	Standard deprotonation enthalpy (kJ/mol) and pK_A (exp. value) [91]	Calculated vertical deprotonation energy (eV)	Adsorption energy on Zn–ZnO (eV), ΔE_{DFT} (ads)	Zn–OCO bond length (Å)
1	HCOOH, Formic (methanoic) acid	0	1444 and 3.74	3.02	−1.62	1.98 and 1.99
2	CH_3–COOH, Acetic (ethanoic) acid	1.5	1458 and 4.76	3.16	−1.61	1.97 and 1.98
3	CH_3–CH_2–COOH Propionic (propanoic) acid	2.6	1453 and 4.86		−2.11	
4	CH_3–C_2H_4–COOH Butyric (butanoic) acid	3.9	1448 and 4.83		−2.07	
5	CH_3–C_3H_6–COOH Valeric (pentanoic) acid	5.3	4.82		−2.08 (−1.48)	
6	CH_3–C_4H_8–COOH Caproic (hexanoic) acid	6.4	4.88		−2.05 (−1.47)	
7	CH_3–C_5H_{10}–COOH Enanthic (heptanoic) acid	7.8		3.39	−2.04 (−1.52)	
8	CH_3–C_6H_{12}–COOH Caprylic (octanoic) acid	8.9	4.89		−2.03 (−1.49)	
9	CH_3–C_7H_{14}–COOH Pelargonic (nonanoic) acid	10.3	4.96	3.52	−2.08 (−1.43) ((−0.38))	1.98 and 1.98
10	CH_3–C_8H_{16}–COOH Capric (decanoic) acid	11.7		3.58	−2.14	

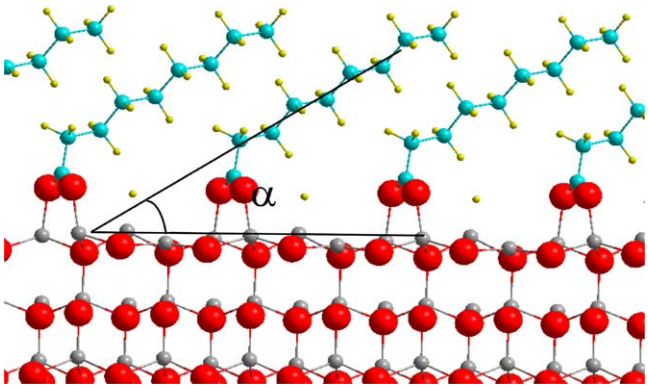

Scheme 1. Definition of the tilt angle α of the molecule to the surface.

layers were let free to relax. We have calculated a relaxation of −0.11 Å for the top surface Zn layer and +0.08 Å for the underlying O layer. More details are given in Ref. [42]. Due to the polar nature of this surface, a spurious charge transfer occurs from the bottom O plane to the Zn plane. This method-related inconsistency was recently counterbalanced by healing the bottom O plane with half-charged H atoms [77]. Tests performed with this method showed no difference in the adsorption energy of the carboxylic acid s. In addition, no dipolar correction (which has to be included for polar molecules as carboxylic acids) could be applied, and therefore this "healing method" was not used in the present work.

Carboxylic acids of formula $CH_3(CH_2)_{n-2}COOH$ (where n = 1–10 is the total number of C atoms in the CA) were considered. They were separately optimized in the same calculation conditions as the ZnO slab. One $CH_3(CH_2)_{n-2}COOH$ molecule adsorbed on a (2×2) supercell of Zn–ZnO(0 0 0 1) surface corresponds to 2.6 molecule/nm^2.

In the following, we refer to as the adsorption mode the mode of adsorption of the carboxylic acid moiety on the surface. In addition, for a given adsorption mode, the angle of the alkyl chain with the surface plane was calculated as shown in Scheme 1.

The energies of interaction/adsorption of carboxylic acid (CA) on the ZnO surface were calculated according to the following equation:

$$\Delta E\ (\text{ads}) = E(\text{CA–ZnO}) - E(\text{CA}) - E(\text{ZnO}), \quad (1)$$

where E(CA–ZnO) is the total energy of the slab including the surface and the CA adsorbed (be it in the molecular or dissociative state), E(CA) and E(ZnO) are the total electronic energies of the CA in vacuum and the ZnO surface, respectively, obtained after separate geometry optimization. ΔE (ads) is given in eV/CA in the used cell.

The electronic properties such as XPS and DOS analyses were performed on the optimized structures. Cls core levels were calculated for C atoms in the framework of the initial state approximation, as explained in Ref. [78]. Indeed the initial state approximation accounts satisfactorily for core level shifts of light elements, as shown recently for e.g. N1s [79,80] and O1s [81].

2.1. van der Waals interactions

Recently, few studies have appeared in the literature which take into account the dispersion forces in the DFT approach for organic molecules adsorbed on inorganic surfaces [82–88]. The reader may be interested in a review of the present advantages and limits of each method, available in Refs [84] and [85]. In the present study, we have performed the dispersion contribution calculations by using the DFT-D scheme in recently proposed DFT-D approach by Grimme et al. [85]. Note that here the dispersion forces are included during geometry optimization. We note in the following ΔE_{DFT} (ads) (respectively ΔE_{D} (ads)) the contribution of Kohn Sham (respectively dispersion forces) to the adsorption and the total (Kohn Sham and dispersive contributions) adsorption energy is noted as $\Delta E_{\text{DFT-D}}$ (ads).

3. Results and discussion

In the first step, we investigated the adsorption mode of the carboxylate group on the surface by means of standard DFT method. One CA molecule is adsorbed on one out of four Zn atoms of the (2×2) supercell of the Zn–ZnO(0 0 0 1) surface, which corresponds to a 2.6 CA/nm^2 coverage. The CA was placed perpendicular to the surface, the distance between two CA being nearly 6.6 Å, and we are confident that H bonds between adsorbed molecules did not take place. The possible van der Waals molecule–molecule and molecule–surface interactions between the molecules and between the molecules and the surface were not taken into account with this method, allowing us to study exclusively the carboxylate moiety–surface interaction. We considered four different adsorption modes: adsorption of undissociated CA, dissociative unidentate adsorption, dissociative bridging adsorption and dissociative bidentate adsorption. In the following, these adsorption modes are discussed in terms of structural and energetic properties.

3.1. Study of the adsorption mode of CA on the ZnO surface

First, the adsorption of undissociated formic, ethanoic and nonanoic acids on ZnO in a perpendicular orientation to the surface is studied. The adsorption is found to be athermic for the three CAs. We have observed the formation of a Zn–H bond (Zn–H bond length = 2.2 Å), associated with a strong outward relaxation of the Zn atom from 0.6 Å to 0.90 Å out of the O plane (Fig. 1a and b). This Zn–H bond formation is likely to be the first step of the carboxylic acid dissociation.

In order to study the dissociative adsorption mode, we have transferred the proton to the neighbouring Zn atom, which corresponds to the unidentate mode of adsorption (Fig. 1c). The second kind of dissociative adsorption mode is a bridging adsorption where the carboxylate groups are bonded to two Zn atoms through Zn–O bonding (Fig. 1d–f). The energies of adsorption (ΔE) for these different adsorption modes were calculated using Eq. (1) as explained in the previous section, and the results are compiled in Table 1. All energies of adsorption are negative, indicating an exothermic process, showing that the stable state of the adsorbed carboxylic acids is the dissociated state, a result in agreement with experimental data reported for the adsorption of acetic and propionic acids on the Zn–ZnO polar surface [64]. It is observed that, for all the carboxylic acids studied (from formic acid to decanoic acid), the bridging adsorption mode is more stable than the unidentate configuration. Here, the carboxylate group is bonded to two Zn atoms (the Zn–O bond length is ≈1.97–1.99 Å, see Table 1), and a Zn–H hydride is formed, a phenomenon already observed [89]. This is also in agreement with our previous result on glycine dissociative adsorption on Zn–ZnO [42]. Note that in the latter case, this configuration was compared with the formation of a surface hydroxyl group (adsorption of the proton on a neighbour surface O atom), but this last configuration was found less stable the one with a surface hydride [89].

Another adsorption mode could be the bidentate configuration where the carboxylate group is bonded to the surface Zn atom as shown in Fig. 1g. For this kind of adsorption mode, adsorption of the nonanoic acid was studied. It was observed that the bidentate adsorption mode is less exothermic than the bridging configuration (ΔE (ads) = −0.38 eV and (ΔE (ads) = −2.10 eV respectively, Table 1).

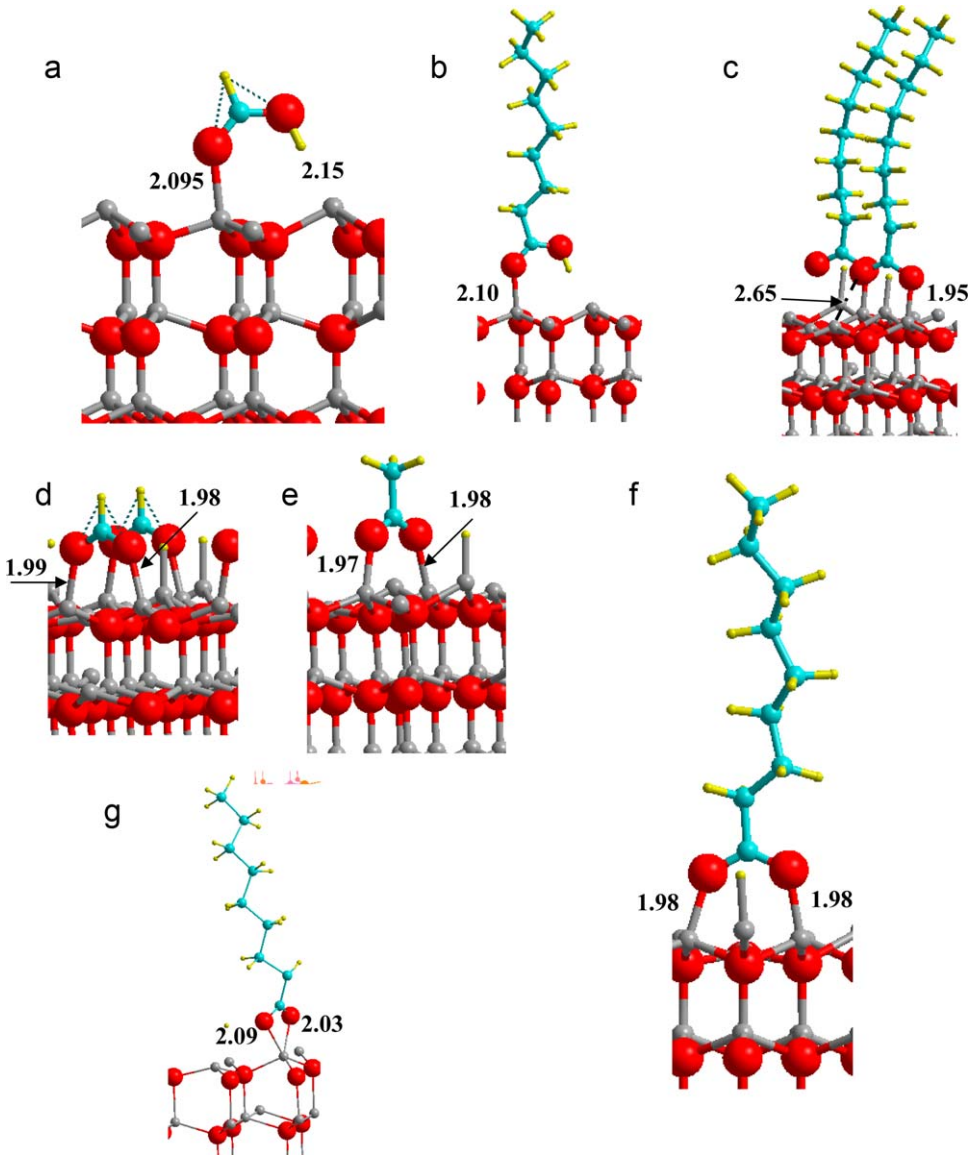

Fig. 1. Geometry optimized structures obtained at the DFT level for CA adsorbed on the Zn–ZnO surface: non dissociative, unidentate adsorption of (a) formic (and (b) nonanoic acids; (c) unidentate dissociative adsorption mode for the nonanoic acid; dissociative bridging adsorption mode for the (d) formic, (e) ethanoic and (f) nonanoic acids; (g) bidentate adsorption mode. The H, product of dissociation, is adsorbed on a surface Zn atom.

As the bridging adsorption mode is more exothermic than the uni-dentate and bi-dentate ones, we conclude that the most likely mechanism for the adsorption of carboxylic acids on the ZnO surface is dissociative bridging adsorption.

3.2. *Influence of the aliphatic chain length on the iono-covalent bond*

Table 1 reports the energies of adsorption ΔE calculated for CA of increasing size, in the dissociative bridging adsorption mode. It is found that the adsorption energy decreases from the formic acid (−1.62 eV) to the propionic acid (−2.11 eV) and then reaches a plateau. We observe a slight tilt of the alkyl chain during optimization. A complete study of the chain tilt is provided in the next part of this study. It is interesting to note that there is no significant difference in the Zn–O bond lengths (≈1.97–1.99 Å in all cases, see Table 1) formed during adsorption of CA with different chain lengths. It is observed that the energy of adsorption decreases with decreasing acidity of the carboxylic acid (the deprotonation energies under the gas phase and pK values are reported in Table 1), from formic and acetic acids to propionic acid, then reaches a plateau. Actually, formic acid is more acidic than butanoic, propionic and acetic acids, with experimental standard enthalpy of deprotonation of 1444, 1448, 1453 and 1458 kJ/mol under the gas phase respectively [91]. Complementary calculations of the vertical deprotonation energies (VDE) confirmed that with increasing chain size, the proton affinity of the anionic species increased (Table 1). Thus, the basicity of the conjugate base $CH_3(CH_2)_{n-2}COO^-$ increases with the increasing size of the acid, explaining the increased binding with the surface. However, no clear effect with the chain size on the adsorption energy is observed for CA larger than propionic acid. Indeed the dependence of acidity with CA chain length under the gas phase is not directly related to acidity in liquid phase [90,91].

Here we have shown that (i) the binding mode of the CA with the ZnO surface is not chain-size dependent and (ii) the energy of the iono-covalent bond with the surface does not vary significantly with the chain length for $n > 2$.

Table 2
Calculated core level shift ΔEB (eV) between the carboxylic/carboxylate C atom and the aliphatic C atoms, for the CH_3–C_7H_{14}–COOH molecule in the gas phase, and in the bridging adsorbed state on the Zn–ZnO(0 0 0 1) surface. The calculations were performed under the initial state approximation.

$\Delta EB = EB(\underline{C}OO(H) - EB(\underline{C}(H))$	ΔE_{VASP}	ΔE_{exp}
Isolated molecule	+3.55	+4.1 [92], +4.9 [32], −5.0 to −5.5 [93]
Adsorbed molecule bridging (carboxylate)	+3.6	+3.3 [32], +3.8 [94]
Adsorbed molecule unidentate (carboxylic)	+3.3	–

3.3. Electronic properties

3.3.1. Core level shifts analysis

In the case of the nonanoic acid, the core level shifts of the C1s in the isolated carboxylic acid were calculated and compared to that of the aliphatic carbons in the chain. The results are summarized in Table 2. For the isolated molecule, we note that the C1s binding energy of the carboxylate carbon COOH is +3.55 eV higher than that of the aliphatic carbon ($\Delta E_{BE}(\underline{C}OOH–\underline{C}H)_{VASP}$ = 3.55 eV). This result is in qualitative agreement with experimental studies which report a shift of +4.1 to +5.5 eV for COOH as compared to the aliphatic carbon ($\Delta E_{BE}(\underline{C}OOH–\underline{C}H)_{exp}$ = +4.1–5 eV) [32,92,93].

In the adsorbed configurations, we have observed that when the nonanoic acid is bonded in the bridging configuration the shift is +3.6 eV (($\Delta E_{BE}(\underline{C}OO–\underline{C}H)_{VASP}$ = +3.6 eV), in good agreement with the experimental value of +3.8 eV measured for acetic acid adsorbed on TiO_2 [94]. This value is also in agreement with another report of +3.3 eV for the anionic COO^- of trimesic acid on Cu(1 1 0) [32]. In the unidentate configuration, the calculated shift from the carboxylate anion to the aliphatic carbon is slightly lower, $\Delta E_{BE}(\underline{C}OO–\underline{C}H)_{VASP}$ is +3.3 eV. To the best of our knowledge, there are no available experimental values for this mode of adsorption.

This result suggests that, in absence of any contamination, XPS can help to discriminate between the unidentate and bridging adsorption modes of carboxylate on the ZnO surface.

3.3.2. DOS analysis

We have investigated the electronic properties of adsorbed ZnO surfaces by calculating the density of states (DOS). For comparison, we have calculated the DOS of bulk ZnO and bare ZnO(0 0 0 1) surface too. The total DOS and projected DOS are shown in Fig. 2. In all cases, 0 eV corresponds to the Fermi level. The (DOS) of ZnO crystal,

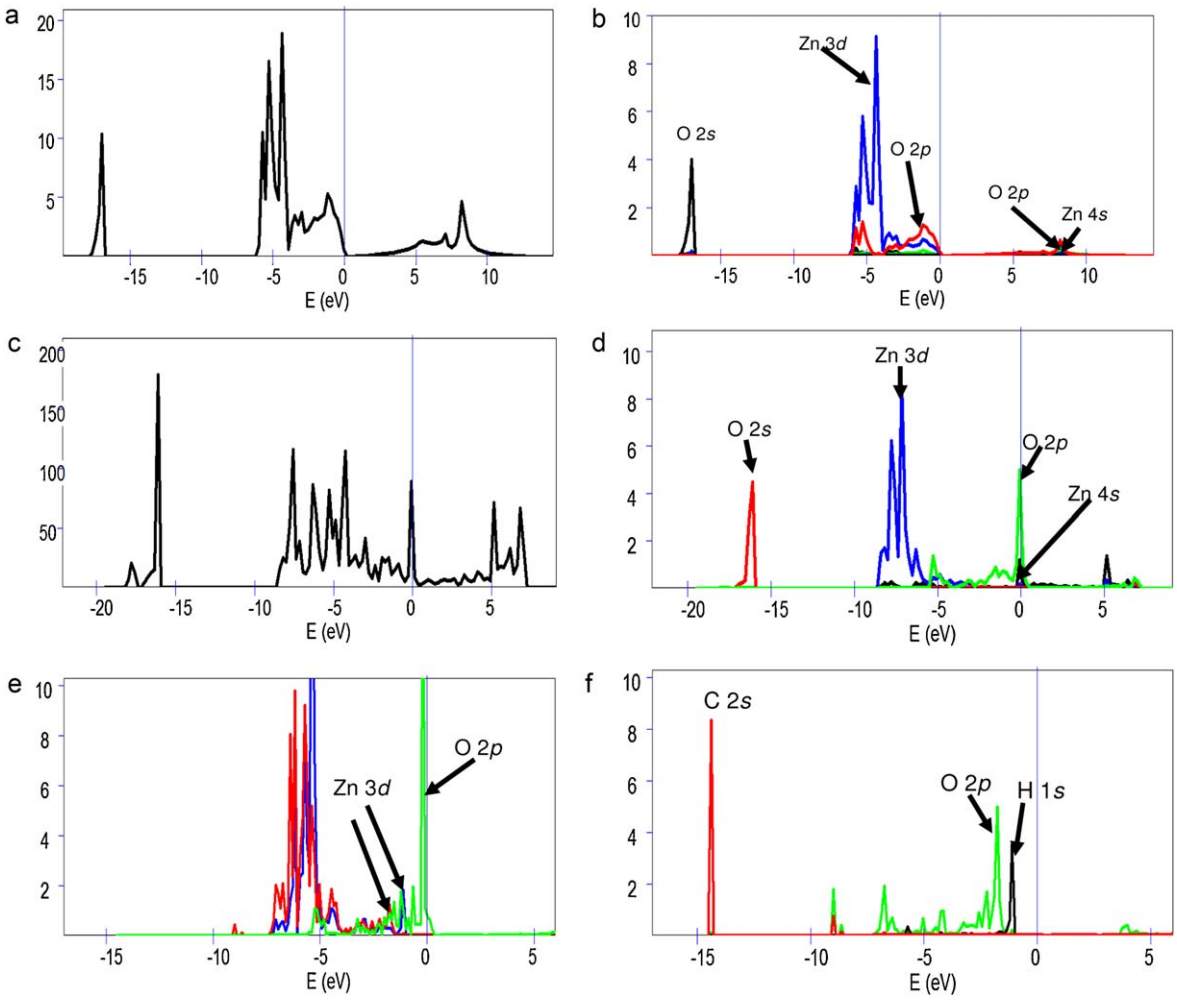

Fig. 2. Density of states (DOS) of bulk ZnO, Zn terminated ZnO(0 0 0 1) surface and adsorbed surfaces. (a) Total DOS and (b) projected DOS of bulk ZnO. (c) Total DOS and (d) projected DOS of Zn terminated ZnO(0 0 0 1) surface. (e, f) PDOS of carboxylic acid adsorbed on the Zn terminated ZnO(0 0 0 1) surface through the bridging attachment, where (e) the PDOS of surface Zn 3*d* and O 2*p* states and (f) the orbitals of adsorbed molecule.

as shown in Fig. 2(a) and (b), reveal that the valence band (VB) is mainly composed of O 2*p* and Zn 3*d* states, with a little contribution of Zn 3*p* states. These are in well accord with the ultraviolet photoemission spectroscopy of ZnO which shows the locality of Zn-3*d* core level below the Fermi energy whereas the VB state is composed of mostly the oxygen *p*-orbital character [95,96]. The conduction band is composed of O 2*p* and Zn 3*p* states. The large peak at −16.9 eV is contributed mainly by O 2*s* orbital. While the contribution of the lowest conduction bands (CBs) is almost fully from Zn 4*s* states.

The density of states of the Zn–ZnO(0 0 0 1) surface (Fig. 2c and d) reveals that there are presence of surface states around the Fermi level which reduce the band gap. This shows an indication of strong surface excitons with a shift in energy below the bulk band gap. The surface states above the Fermi level arise from O 2*p* and Zn 4*s* orbitals as shown in Fig. 2d, which give a metallic character. This is in agreement with the electronic structure of the ZnO(0 0 0 1) surface by angle-resolved photoelectron spectroscopy (ARPES) where the surface states are interpreted as the 'back-bondings' of the Zn 4*s*–O 2*p* mixed bulk states [97].

For the adsorbed structures, the DOS were calculated for two different types of adsorption on the ZnO surface such as adsorption of uni-dentate and bridging adsorption of carboxylic acid. The qualitative features of DOS for both of these adsorption modes are similar. For simplicity, here we discuss only the DOS of bridging adsorption mode as illustrated in Fig. 2(e) and (f). As the chain size does not have any significant effect on the energy of adsorption, here we have employed adsorption of CH_3–C_7H_{14}–COOH on the ZnO surface for the DOS investigation.

Similar to the bare surface, the surface states around the Fermi level are mainly contributed by the surface O 2*p* orbitals (green curve of Fig. 2e). (For interpretation of the references to color in the text, the reader is referred to the web version of the article.) Besides these, the presence of adsorbed molecular levels is evident in HOMO and LUMO. The VB is contributed by H 1*s* and O 2*p* orbitals of the –COOH group. It is interesting to note that the bonding features are clearly evident in the electronic structure. The small peak at –1.1 eV (blue curve of Fig. 2e) corresponds to the Zn 3*d* orbitals which is associated with the H 1*s* peak (black curve of Fig. 2f). It shows the Zn–H bonding on the surface due to the proton transfer after carboxylic acid dissociation. The peak at −1.7 eV (green curve of Fig. 2f) corresponds to the O 2*p* orbitals of carboxylic group which is associated with the small Zn 3*d* peak of the surface. It clearly shows the Zn–O bonds formed due to the adsorption of CA molecules on the surface. An extra peak between −14.20 eV and −14.70 eV is mainly composed of 2*s* orbital of carbon atom of the aliphatic chain. The CB is contributed by C 2*p* states of the carboxylic group (not shown in the figure).

In the preceding paragraphs, we have studied the pure chemical bonds formed between the CA and ZnO surfaces. In the following, we investigate the contributions of dispersion forces on the adsorption and self assembling properties. We have first analyzed the vdW contributions when adsorption occurs in absence of lateral interactions, then the influence of vdW interactions on the geometry and adsorption energy is studied. A particular attention is devoted to the tilt angle between the alkyl chain and the surface.

3.4. van der Waals interactions and self assembling

3.4.1. Contribution of van der Waals forces in adsorption at low coverage

Here we aim to investigate the dispersion contribution on the molecule–surface interaction. To this end, one nonanoic CA is adsorbed on a (6 × 2) cell in order to avoid any lateral interaction in the *x* direction and study the influence of the orientation of the molecule to the surface without lateral interaction. The molecule is adsorbed on the Zn–ZnO surface in the bridging bidentate mode.

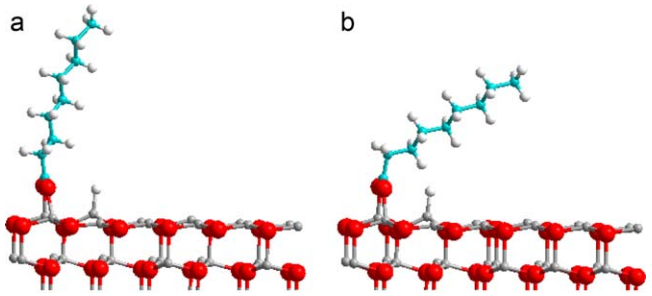

Fig. 3. Geometry optimized structures obtained at the DFT-D level for the nonanoic acid adsorbed on the Zn–ZnO surface at low coverage (6 × 2 cell).

Fig. 3 shows the two configurations considered, one perpendicular to the surface and another one tilted with respect to the surface with a tilt angle of 35° (see the definition in Scheme 1). These two configurations are iso-energetics at the DFT level (ΔE = 0.04 eV) and the tilted configuration is slightly more stable than the perpendicular one at the DFT-D level (ΔE = +0.04 eV) and at the DFT level (ΔE = +0.13 eV)). We note that the geometries obtained after optimization at the DFT and DFT-D levels are very similar, including the tilt angle to the surface. The total energy of adsorption is −2.55 eV for the perpendicular orientation and −2.68 eV for the tilted configuration, including dispersion force contributions to the adsorption energy which account for −0.18 eV and −0.31 eV for the perpendicular and tilted orientations respectively. It shows that (i) at low coverage, dispersion represents 8–11% of the total adsorption energy; (ii) the dispersion forces interaction of the CA with the surface in the tilted orientation is not significant enough to induce a determined angle of adsorption. This result suggests that (i) the molecule is rather flexible at the surface and that deformation cost to modify the tilt angle will be negligible, thus a certain disorder at the surface at low coverage is to be expected, (ii) for this chain size, the van der Waals interaction of the molecule with the surface is not large enough to be of significant contribution in the adsorption, (iii) the formation of the iono-covalent bond with the surface is the driving force for adsorption. Obviously, van der Waals forces are expected to play an important role in self-assembling at the surface as is described in the next paragraph.

3.4.2. Geometry and energetics of SAM formation

Now, we study the influence of the van der Waals forces on the chain orientation and energetic at the same coverage, 2.6 molecule/nm^2, a coverage at which SAMs may form at the surface. Indeed, a simple examination of the constraints imposed by the surface (COO anchoring on two Zn atoms) shows that the COO–COO distance between two neighbouring CA is 6.6 Å. This distance is larger than the distance of 4.45–4.6 Å found in auto-assemblies of alkyl chains and paraffins which arrange in a pseudohexagonal closed packed layer structure [47,98]. Therefore, as shown in [47], to optimize lateral interactions between the alkyl chains, a tilt of the chains to the surface is possible.

3.4.2.1. Case of hexanoic and nonanoic acids. A systematic study of the adsorption of CA as a function of the tilt angle was performed for two sizes of molecules, *n* = 6 and 9. Fig. 4 shows the geometries obtained at the DFT-D level for the hexanoic and nonanoic acids adsorbed at tilt angles of 90, 60, 45 and 30° to the surface and Fig. 5a reports on the energies of the different orientations with respect to the perpendicular orientation for the nonanoic acid.

We observe that the first C atom of the alkyl chain remains located on top of the COO moiety, and that bending occurs for the next C atoms. The final angles of the alkyl chains to the surface are reported in Table 3. Whatever the starting angle of the alkyl

Table 3
Adsorption energies (total and van der Waals contributions), energy differences (total and van der Waals contributions) between the tilted and perpendicular structures, orientations of the molecules to the surface, and DFT-D adsorption energies, for the CA of increasing chain length adsorbed on ZnO.

Chain length (n)	Formula	α		$\Delta E_{\text{DFT-D}}$ (ads)	$\Delta\Delta E_{\text{DFT-D}}$ (tilted − perp)*	ΔE_{D} (ads)	$\Delta\Delta E_{\text{D}}$ (tilted − perp)*
		Initial	Final				
3	CH_3–CH_2–COOH Propionic	90	$\alpha = 90$	−2.46		−0.35	
	(propanoic) acid	45	$\alpha = 47$	−2.43	+0.03	−0.34	0.04
4	CH_3–C_2H_4–COOH Butyric	90	$\alpha = 90$	−2.44		−0.37	
	(butanoic) acid	60	$\alpha = 53$	−2.42	+0.02	−0.37	0
5	CH_3–C_3H_6–COOH Valeric	90	$\alpha = 88$	−2.49		−0.38	
	(pentanoic) acid	35	$\alpha = 37$	−2.46	+0.03	−0.41	−0.035
6	CH_3–C_4H_8–COOH Caproic	90	$\alpha = 87$	−2.53		−0.37	
	(hexanoic) acid	60	$\alpha = 62$	−2.53	−0.02	−0.39	−0.06
		45	$\alpha = 46$	−2.53	−0.03	−0.39	−0.02
		30	$\alpha = 35$	−2.53	−0.001	−0.47	−0.12
7	CH_3–C_5H_{10}–COOH	90	$\alpha = 85$	−2.49		−0.36	
	Enanthic (heptanoic) acid	30	$\alpha = 35$	−2.59	−0.1	−0.55	−0.19
8	CH_3–C_6H_{12}–COOH Caprylic	90	$\alpha = 85$	−2.51		−0.37	
	(octanoic) acid	30	$\alpha = 36$	−2.63	−0.25	−0.60	−0.23
9	CH_3–C_7H_{14}–COOH	90	$\alpha = 85$	−2.53		−0.36	
	Pelargonic (nonanoic) acid	60	$\alpha = 59$	−2.65	−0.12	−0.39	−0.05
		45	$\alpha = 51$	−2.66	−0.13	−0.46	−0.1
		30	$\alpha = 34$	−2.77	−0.24	−0.69	−0.35

*$E_{\text{tilted}} - E_{\text{perp.}}$
α, angle of the alkyl chain with the surface (see Scheme 1).

chain to the surface, only a slight variation is found during geometry optimization. For the nonanoic acid, the chain–chain distance decreases with decreasing tilt angle to the surface from 6.6 Å in the perpendicular configuration to 5.1, 5.0 and 3.8 Å for the 60, 45 and 35° tilt to the surface respectively. In the most tilted configuration, we observe that H atoms point towards the C of the neighbouring alkyl chain, thus minimizing the C–H distances to 2.7–3.2 Å range, and achieving a zip-like assembly. Also, in this configuration, H–H distances are now 2.1–2.6 Å. All those distances are clearly typical of weak interactions. Indeed, Fig. 5a evidences that for the nonanoic acid, the van der Waals contribution to the adsorption energy decreases from −0.4 to −0.7 eV with decreasing angle to the surface, indicating a stabilization by van der Waals interactions between the adsorbed molecule.

Comparing the total energies at DFT-D method (Fig. 5b), we observe that even if the energy differences of the various configurations belong to a narrow interval of 0.3 eV, the systematic study allows to drive a trend for stabilization of the nonanoic acid adsorption by decreasing the tilt angle to the surface. In strong contrast with what observed for the nonanoic acid, all configurations are isoenergetic for the hexanoic acid.

To summarize, we find that, the inclusion of van der Waals forces stabilizes the tilted configuration of the nonanoic acid to the surface whereas no effect is found for the hexanoic acid. The most stable

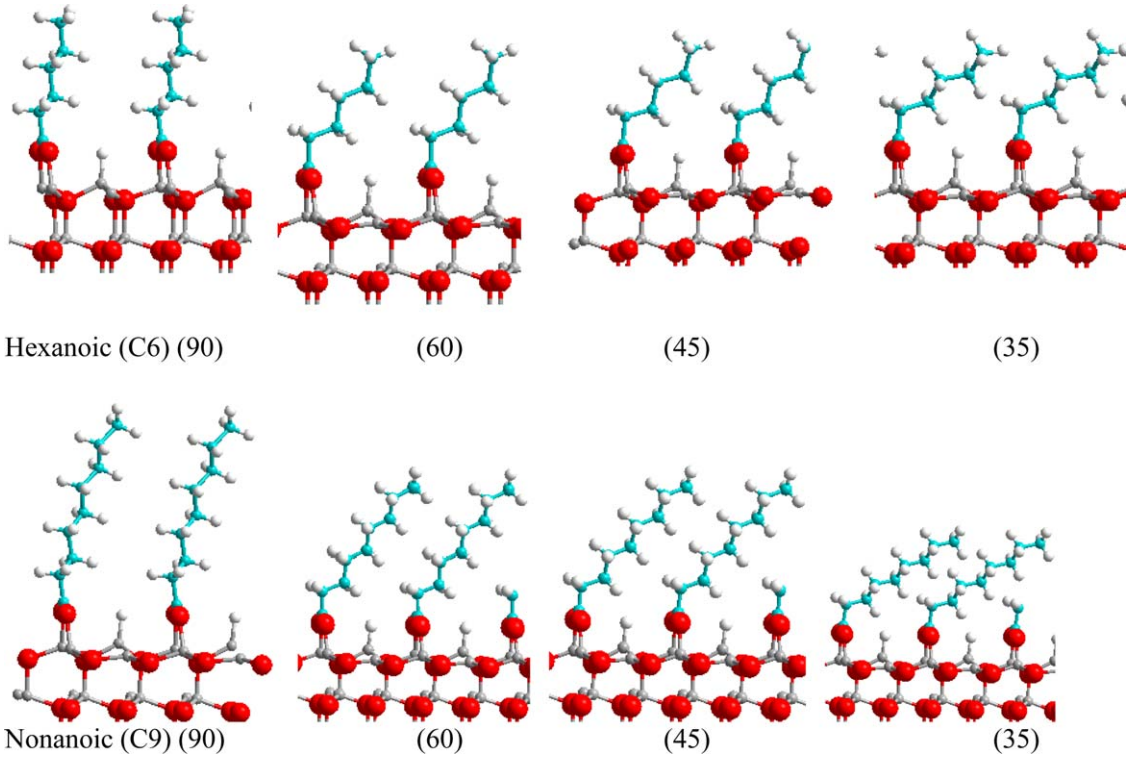

Fig. 4. Geometry optimized structures obtained at the DFT-D level for the hexanoic and nonanoic acids adsorbed on the Zn–ZnO surface for different angles with the surface.

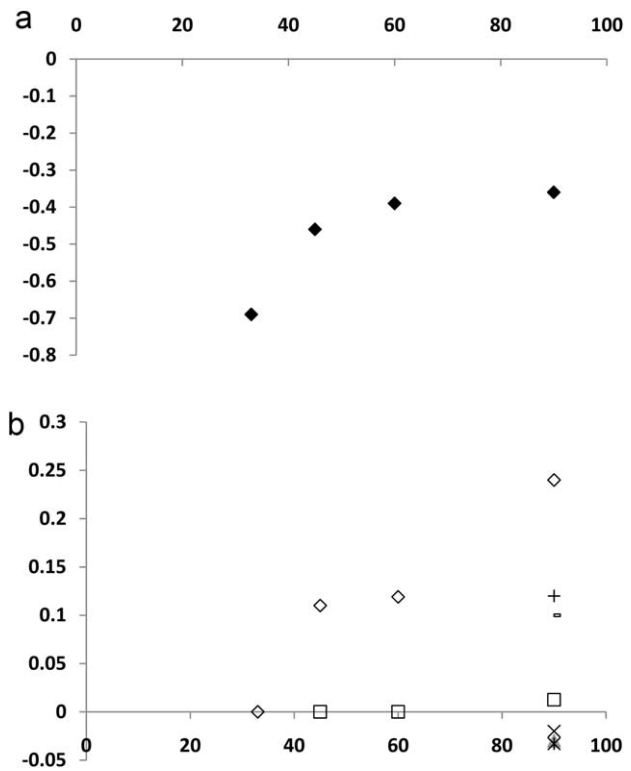

Fig. 5. Variation of energetic data as a function of the tilt angle to the surface for the hexanoic and nonanoic acids (CH_3–$(CH_2)_4$–COOH and CH_3–$(CH_2)_7$–COOH): (a) dispersion contribution to the adsorption energy (ΔE_D (ads)) for the nonanoic acid as a function of α. (b) Variation of the total energy of adsorption ($\Delta\Delta E_{DFT\text{-}D}$ (ads)) (eV) as a function of the tilt angle to the surface α (°) (the reference is the most stable state, with $\alpha = 35°$), for the nonanoic acid (rhombus) and the hexanoic acid (squares).

configuration is achieved for a tilt angle of 35° to a surface, We just mention that this important tilt was found stable during a 1 ps long ab initio MD run at 700 K.

3.4.2.2. Other chain lengths. In Fig. 6, the optimized geometries of the tilted (starting from $\alpha = 30°$) molecules adsorbed at the ZnO surface, obtained at the DFT-D level with increasing molecule sizes ($n = 3$–9), are shown and quantitative data are reported in Table 3. The molecules in the perpendicular orientation are not shown as there is no significant change as compared to the DFT geometry. We observed that the tilt angle to the surface (starting from the value of 30°) does not vary with the chain length and achieves a value of 34–37° for all molecules (Fig. 6a).

In Fig. 6b and Table 3, the adsorption energies of the tilted and perpendicular structures are reported for increasing chain length. In the perpendicular orientation, the adsorption energy is comprised in a narrow interval (−2.46 and −2.53 eV) and no significant decrease of adsorption energy with increasing chain size is identified. In contrast, in the tilted orientation, there is a net decrease of the adsorption energy with increasing chain length (from −2.43 eV to −2.77 eV for $n = 3$–9), evidencing the role of attractive lateral interactions between the molecules. For the smallest CA, the perpendicular orientation is more stable than the tilted one, because no lateral interaction occurs by bending. With the increase of molecule size, a increase in the lateral interactions may take place. The results also suggest that the perpendicular/tilted transition can occur for a CA size of $n = 7$ C atoms (heptanoic acid). Such a change in the tilt angle to the surface with the molecule size was already observed for thiols on gold [99].

We also notice that the dispersion contribution to the adsorption energy in the perpendicular orientation does not vary with the size of the molecule and is ≡0.35–0.38 eV. In the tilted orientation, the vdW contribution to adsorption energy decreases from −0.34 ($n = 3$) to −0.69 ($n = 9$) eV, again evidencing that the stabilization of this structure is due to van der Waals forces only.

To summarize, we have shown that a transition perpendicular/tilted orientation to the Zn–ZnO(0 0 0 1) surface is achieved for CA larger than the hexanoic acid, thanks to intermolecular van der Waals interactions, and that the SAM formed has a tilt angle of 35° to the surface.

3.4.3. Electronic analysis of the SAM structure

The electronic properties investigation on the SAM structure obtained from the DFT-D method is performed by DOS calculation. The DOS figures are illustrated in Fig. 7. There is no major qualitative difference between the DOS obtained with DFT and DFT-D methods. As in the case of DFT approach, the total DOS at the DFT-D (Fig. 7a show the presence of occupied surface states in the Fermi level. All the small peaks between −9.0 eV and −15.5 eV are contributed by 2*p* states of C atom belonging to the –COOH group (Fig. 7b)). The VB is contributed by Zn 3*d* (blue curve of Fig. 7e) and O 2*p* (green curve of Fig. 7d) states, whereas the CB is mainly contributed by C 2*p* and O 2*p* (green curve of Fig. 7(b) and (d)) of –COOH group. (For interpretation of the references to color in the text, the reader is referred to the web version of the article.) The surface states are mainly contributed by O 2*p* states (green curve of Fig. 7d), similar to that observed in the case of DFT approach. The H 1*s* peak at –1.85 eV in the VB (black curve in Fig. 7c) is associated with the sharp peak of Zn 3*d* orbitals, which shows a Zn–H bonding at the surface due to the proton transfer after carboxylic acid dissociation.

3.5. Conditions of SAM formation on ZnO

Here, we have quantified the role of van der Waals forces on self assembling. In this way, we have investigated the driving forces controlling adsorption and the effect of adsorbate–adsorbate interactions on the chemisorption at the surface.

In the preceding paragraphs, we have shown that the van der Waals interaction of the molecule with the surface does not play a determining role in the proper binding energy to the surface, which is driven by the formation of ionocovalent bonds. In contrast, even for the small chain lengths investigated here, van der Waals forces account for cohesion in the adsorbed layer and orientation of the layer towards the surface. In consequence, the adsorption energy decreases with increasing chain length, a trend in agreement with that observed experimentally for thiols adsorption on Au [100].

From our results, we may now propose conditions for SAM formation on ZnO(0 0 0 1)

- First, a strong ionocovalent bond to the surface has to be formed. In the case of ZnO, the bridging configuration is possible because the Zn–Zn (3.3 Å) distance at the surface is compatible with the O–O distance in the COOH molecule (2.28 Å). However, it is interesting to notice that strong bonds may also be formed through unidentate adsorption e.g. on Al_2O_3 surfaces, where the Al–Al distances are too long to accommodate a bridging adsorption [31].
- Second, as the molecules' molecules anchoring head–head distances are monitored by the surface constraints, the chain–chain distance imposed by the surface crystallography does not allow to optimize the lateral interactions. Here the 6.3 Å distance is longer than the expected 4.4 Å distance between alkyl chains in molecular crystals [47]. In consequence, the molecules adopt a tilted orientation to the surface. A simple calculation allows to deduce

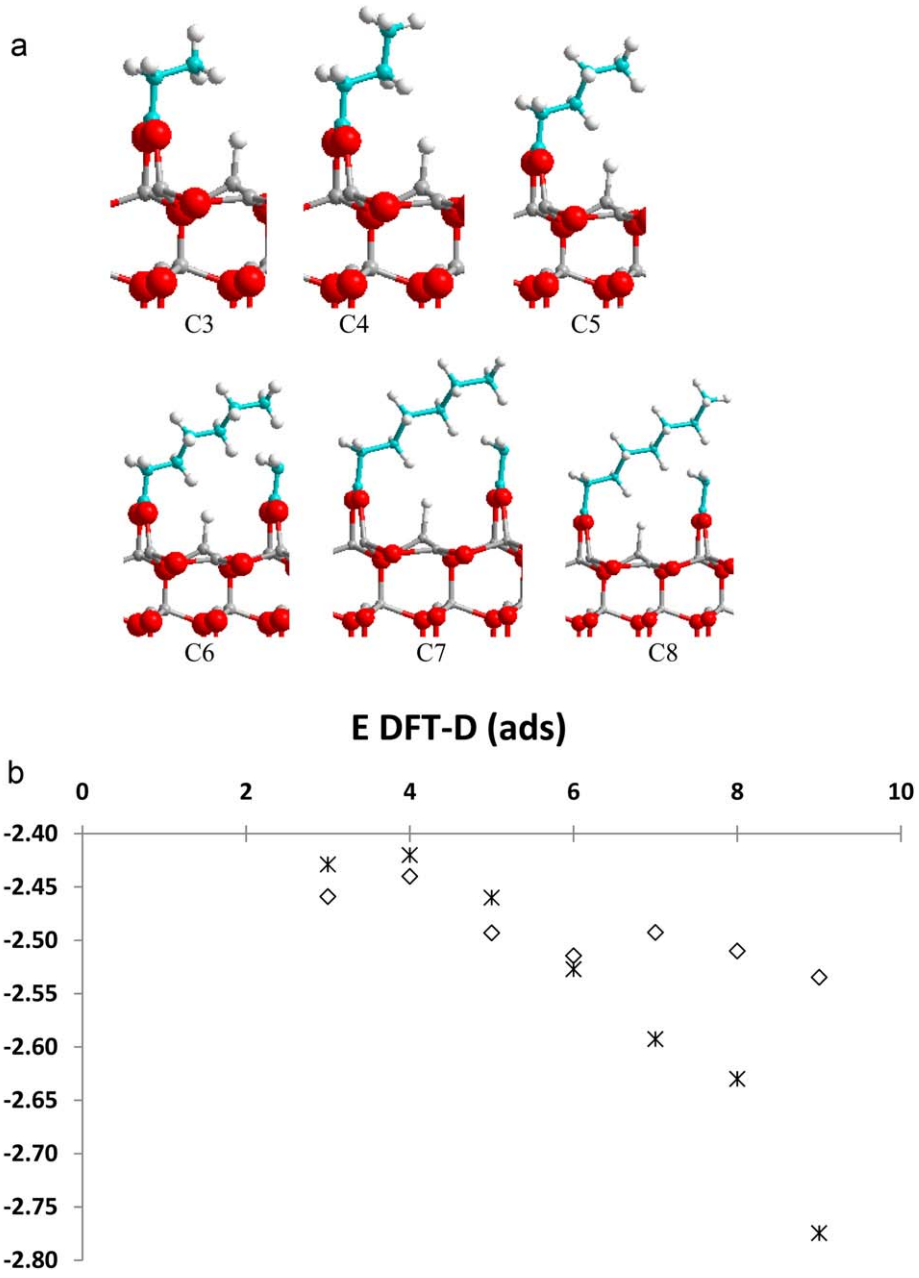

Fig. 6. Geometry optimized structures obtained at the DFT-D level for the carboxylic acids of increasing chain length on the Zn–ZnO(0 0 0 1) surface in the tilted ($\alpha = 35^\circ$) configuration: (a) optimized geometries; (b) adsorption energy ($\Delta E_{\text{DFT-D}}$ (ads) (eV) in the perpendicular orientation to the surface (◊) and in the tilted orientation ($\alpha = 35^\circ$) (*) to the surface.

the value of the tilt angle α: if R is the cation–cation distance at the surface, α the tilt angle to the surface, and l the distance between two neighbouring chains, l has the optimized value of 4.4 Å for $\alpha = \text{arc sin } l/R$. In the case of the Zn/ZnO(0 0 0 1) surface, $\alpha = 41^\circ$, a value close to 35° found in our calculations. The slight discrepancy found may be due to the small size of the chains studied here (in fact, the molecule–molecule distances in closed packed arrangements of alkyl molecules increases with the size [47]).

- Third, the molecule has to be large enough so that the bending to the surface allows lateral interactions. For a $CH_3–(CH_2)_{n-2}–COOH$ adsorbed at the surface, the tilted alkyl chain contains $(n-1)$C atoms and has a length of $L = 2.57\ [(n-2)/2]$, where 2.57 Å is the length of a $(CH_2)_2$ unit. To form interactions with the neighbouring CA alkyl chain, the following condition has to be verified: $L\cos\alpha > R$. Taking the obtained value of 35°, we find $n > 6$.
- Finally, the best chain–chain interaction is achieved for structures tilted in order to optimize H–C attractions, as observed here for the nonanoic acid.

As a final remark, we have to mention that in the present work, we have considered the chain length and tilt angle only. Other in the *yz* plane were investigated, other important parameters such as lean angle of molecules in the *xz* plane, reorientation of the CH_2 along the chain axis, and possible substructure formation were not considered. However, the interesting results found here are encouraging to explore these other parameters.

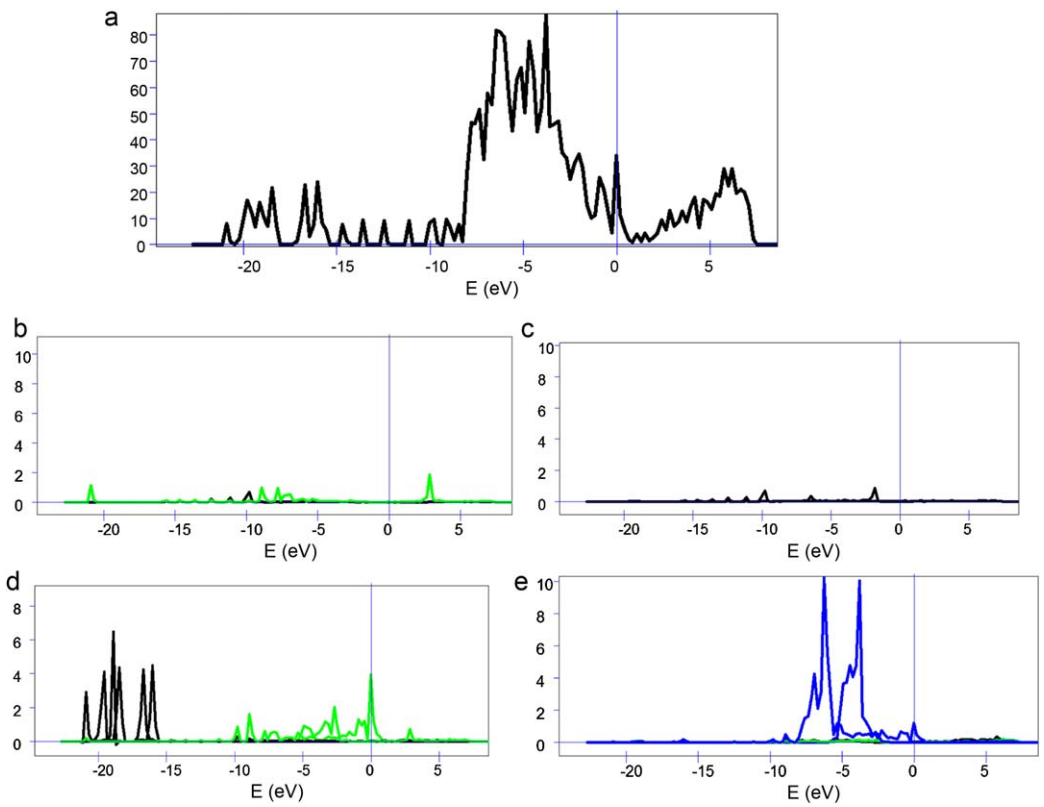

Fig. 7. DOS of the SAMs formed on ZnO surface obtained with DFT-D method: (a) total DOS, (b) PDOS of carbon, (c) PDOS of H, (d) PDOS of Zn and (e) PDOS of O. The black, green and blue curves represent *s*, *p* and *d* orbital states.

4. Conclusion

The study of the interaction of carboxylic acids (CA) of increasing size with a model oxide surface, Zn–ZnO(0 0 0 1) was performed by DFT. Considering the CA/ZnO interaction, (adsorption in a perpendicular orientation to minimize lateral interactions), the binding mode of carboxylic acids with the Zn–ZnO surface is independent on the aliphatic chain length, the favoured mode of adsorption being the dissociative, bridging one, where one cycle Zn–O–C–O–Zn is formed. The energy of interaction of the carboxylic acids with the surface increases with the increasing chain length, for $n = 0$–2 aliphatic carbons (formic, ethanoic acids), then reaches a plateau for a chain of aliphatic from $n = 2$–9 carbons (propionic acid to decanoic acid). This trend is in agreement with the known decrease of acidic character of carboxylic acids with increasing size, confirming the acid–base character of the interaction.

The van der Waals interactions between molecule and surface are weak and account for 10% of the energy of adsorption or less, be it in a perpendicular or tilted orientation. In contrast, van der Waals forces play a significant role in the lateral chain–chain interactions and explain the tilted orientation of the molecules with respect to the surface. Because of the rather small size of the molecules studied here, a rather large bending angle of 35° to the surface (56° to the normal of the surface) is found, which maximizes lateral van der Waals interactions. In consequence, the tilted orientation, the energy of adsorption decreases with the increasing chain length, indicating an enhanced exothermic process with chain length. In fact, whereas adsorption itself is due to a strong ionocovalent bond with the ZnO surface, further stability is gained through self-assembling of the alkyl chains. The bending allows to optimize the chain–chain distance and a C–H–C repartition in the interactions. Finally, whereas the tilted and perpendicular orientations are nearly isoenergetics for chains of small length, $n < 6$, for larger chains our results indicate that all chains will be tilted. These results also explain why ordering increases with the molecule size.

The DOS investigation illustrates the two important features of the adsorption: the formation of Zn–H bonding on the surface due to the proton transfer after carboxylic acid dissociation and the formation of Zn–O bond. C1s calculated core level shifts suggest that XPS could help to discriminate between the unidentate and bridging adsorption modes.

Acknowledgements

The national calculation centres CINES and IDRISS are thanked for calculation time (project x2011082217). The reviewers are thanked for their very fruitful scientific remarks.

References

[1] W. Funke, J. Coating. Technol. 55 (1983) 31–38.
[2] S.M. Cohen, Corrosion 51 (1995) 71–78.
[3] J.G.N. Thomas, A.D. Mercer, A.D. Mercer, Organic Inhibitors of Corrosion of Metals, Yurii I. Kuznetsov (Ed.), second ed., Illustrated, Springer, 1996, 283 pp.
[4] B. Müller, React. Funct. Polym. 39 (1999) 165–177.
[5] J. Van Den Brand, S. Van Gils, P. Beentjes, H. Terryn, V. Sivel, J.-H. De Wit, Prog. Org. Coat. 51 (2004) 339–350.
[6] R. Posner, K. Wapner, M. Stratmann, G. Grundmeier, Electrochim. Acta 54 (2009) 891.
[7] I. Yu, K. Kuznetsov, A. Ibatullin, Prot. Met. 38 (2002) 439–444.
[8] M. Frey, S. Harris, J. Holmes, D. Nation, S. Parsons, P. Tasker, R. Winpenny, Chem.-Eur. J. 6 (2000) 1407–1415.
[9] Z. Lu, Y. Qiu, X. Guo, Corr. Eng. Sci. Technol. 44 (2009) 43.
[10] M. Spah, D. Spah, B. Deshwal, S. Lee, Y. Chae, J. Park, Corros. Sci. 51 (2009) 1293.
[11] J. Ai, X. Guo, Z. Chen, Appl. Surf. Sci. 253 (2006) 683–688.
[12] D. Ornek, T. Wood, C. Hsu, Z. Sun, F. Mansfeld, Corrosion 58 (2002) 761–767.
[13] C.-M. Pradier, V. Humblot, L. Stievano, C. Methivier, J.-F. Lambert, Langmuir 23 (2007) 2463.

[14] G.E. Brown, V.E. Henrich, W.H. Casey, D.L. Clark, C. Eggleston, A. Felmy, D.W. Goodman, M. Gratzel, G. Maciel, M.I. Mccarthy, K.H. Nealson, D.A. Sverjensky, M.F. Toney, J.M. Zachara, Chem. Rev. 99 (1999) 77.
[15] R.M. Hazen, D.A. Sverjensky, Cold Spring Harb. Persp. Biol. 2 (2010) A002162.
[16] J. Van Den Brand, O. Blajiev, P. Beentjes, H. Terryn, J. De Wit, Langmuir 20 (2004) 6308–6317.
[17] L. Wang, Y. Fang, Spectrochim. Acta Part A: Mol. Biomol. Spectrosc. 63 (2006) 614.
[18] J. Vohs, M. Barteau, Surf. Sci. 197 (1988) 109–122.
[19] D. Zhang, Q. Cai, L. Gao, K. Lee, Corros. Sci. 50 (2008) 3615.
[20] T. Qiu, M. Barteau, J. Colloid Interface Sci. 303 (2006) 229–235.
[21] H. Ashima, W.-J. Chun, K. Asakura, Surf. Sci. 601 (2007) 1822–1830.
[22] R. Lindsay, S. Tomic, A. Wander, M. Garcia-Mendez, G. Thornton, J. Phys. Chem. C 112 (2008) 14154.
[23] K. Kinoshita, S. Suzukib, W.-J. Chun, S. Takakusagi, K. Asakura, Surf. Sci. 603 (2009) 552–557.
[24] X. Tian, J. Xu, W. Xie, J. Phys. Chem. C 114 (2010) 3973–3980.
[25] L.H. Dubois, R.G. Nuzzo, Annu. Rev. Phys. Chem. 43 (1992) 437–463.
[26] C. Lomenech, G. Bery, D. Costa, L. Stievano, J.F. Lambert, Chemphyschem 6 (2005) 1061.
[27] D. Costa, C. Lomenech, M. Meng, L. Stievano, J.F. Lambert, J. Mol. Struct.-Theochem. 806 (2007) 253.
[28] L. Stievano, Y. Piao, I. Lopes, M. Meng, D. Costa, J.F. Lambert, Eur. J. Miner. 19 (2007) 321.
[29] D. Costa, A. Tougerti, F. Tielens, C. Gervais, L. Stievano, J.F. Lambert, Phys. Chem. Chem. Phys. 10 (2008) 6360.
[30] P.A. Garrain, D. Costa, P. Marcus, J. Phys. Chem. C 115 (2011) 719–727.
[31] C. Arrouvel, B. Diawara, D. Costa, P. Marcus, J. Phys. Chem. C 111 (2007) 18164.
[32] T. Classen, M. Lingenfelder, Y. Wang, R. Chopra, C. Virojanadara, U. Starke, G. Costantini, G. Fratesi, S. Fabris, S. De Gironcoli, S. Baroni, S. Haq, R. Raval, K. Kern, J. Phys. Chem. A 111 (2007) 12589.
[33] J.W. Han, D.S. Sholl, Phys. Chem. Chem. Phys. 12 (2010) 8024.
[34] S. Koppen, O. Bronkalla, W. Langel, J. Phys. Chem. C 112 (2008) 13600.
[35] W. Langel, L. Menken, Surf. Sci. 538 (2003) 1.
[36] G. Grundmeier, M. Stratmann, Annu. Rev. Mater. Res. 35 (2005) 571–615.
[37] N. Biswas, S. Kapoor, H.S. Mahal, T. Mukherjee, Chem. Phys. Lett. 444 (2007) 338–345.
[38] J.M. Delgado, R. Blanco, J.M. Orts, J.M. Perez, A. Rodes, J. Phys. Chem. C 113 (2009) 989–1000.
[39] P.R. Mcgill, H. Idriss, Surf. Sci. 602 (2008) 3688–3695.
[40] M.J. Lundqvist, M. Nilsing, P. Persson, S. Lunell, Int. J. Quantum Chem. 106 (2006) 3214–3234.
[41] D. Costa, P.-A. Garrain, B. Diawara, P. Marcus, Langmuir 27 (2011) 2747.
[42] S. Irrera, D. Costa, P. Marcus, J. Mol. Struct.-Theochem. 903 (2009) 49–58.
[43] C. Mendive, T. Bredow, M. Blesa, D. Bahnemann, Phys. Chem. Chem. Phys. 8 (2006) 3232.
[44] M. Nilsing, P. Persson, L. Ojamae, Chem. Phys. Lett. 415 (2005) 375.
[45] K. Kim, H. Lee, H. Kim, Vib. Spectrosc. 44 (2007) 308–315.
[46] L. Ojamae, C. Aulin, H. Pedersen, P. Kall, J. Colloid Interface Sci. 296 (2006) 71.
[47] A. Ulman, Chem. Rev. 96 (1996) 1533.
[48] S. Ramachandran, Bl Tsai, M. Blanco, H. Chen, Tang Yc, Goddard Wa, Langmuir 12 (1996) 6419.
[49] Whelan Cm, M. Kinsella, Hm Ho, K. Maex, J. Electrochem. Soc. 151 (2004) B33–B38.
[50] D. Allara, R.G. Nuzzo, Langmuir 1 (1985) 45.
[51] D. Allara, R.G. Nuzzo, Langmuir 1 (1985) 52.
[52] H. Ogawa, T. Chihera, K.J. Taya, Am. Chem. Soc. (1985) 107.
[53] Y.T. Tao, J. Am. Chem. Soc. 115 (1993) 4350.
[54] E.L. Smith, M.D. Porter, J. Phys. Chem. 97 (1993) 4421.
[55] A.H.M. Soundag, A.J.W. Tol, F.J. Touwslager, Langmuir 8 (1992) 1127.
[56] W.R. Thompson, J.E. Pemberton, Langmuir 11 (1995) 1720.
[57] M.G. Samart, C.A. Brown, J.G. Gordon, Langmuir 9 (1993) 1082.
[58] E. Torres, A.T. Blumenau, P.U. Biedermann, Chemphyschem 12 (2011) 999.
[59] J.-G. Wang, A. Selloni, J. Phys. Chem. C 113 (2009) 8895–8900.
[60] F. Tielens, V. Humblot, Cm Pradier, Int. J. Quantum Chem. 108 (2008) 1792.
[61] F. Tielens, E. Santos, J. Phys. Chem. C 114 (2010) 9444.
[62] F. Tielens, D. Costa, V. Humblot, C.-M. Pradier, J. Phys. Chem. C 112 (2008) 182.
[63] R.K. Smith, P.A. Lewis, P.S. Weiss, Prog. Surf. Sci. 75 (2004) 1.
[64] C. Woell, Prog. Surf. Sci. 82 (2007) 55.
[65] P. Qiu, D. Persson, C. Leygraf, J. Electrochem. Soc. 156 (2009) C441–C447.
[66] A. Lenz, L. Selegard, F. Soderlind, A. Larsson, P.O. Holtz, K. Uvdal, L. Ojamae, P.-O. Kall, J. Phys. Chem. C 113 (2009) 17332.
[67] C.W. Sheen, J.X. Shi, J. Martensson, A.N. Parikh, D.L. Allara, J. Am. Chem. Soc. 114 (1992) 1514.
[68] J.P. Perdew, J.A. Chevary, S.H. Vosko, K.A. Jackson, M.R. Penderson, D.J. Singh, C. Fiolhais, Phys. Rev. B 46 (1992) 6671.
[69] J.P. Perdew, Y. Wang, Phys. Rev. B 45 (1992) 13244.
[70] G. Kresse, J. Hafner, Phys. Rev. B 49 (1994) 14251.
[71] G. Kresse, J. Furthmuller, Comp. Mater. Sci. 6 (1996) 15.
[72] G. Kresse, J. Joubert, Phys. Rev. B 59 (1999) 1758.
[73] P.E. Blöchl, Phys. Rev. B 50 (1994) 17953.
[74] S. Irrera, D. Costa, K. Ogle, P. Marcus, J. Mol. Struct.-Theochem. 903 (2009) 49.
[75] H.J. Monkhorst, J.D. Pack, Phys. Rev. 13 (1976) 5188.
[76] H. Karzel, W. Potzel, M. Köfferlein, W. Schiessl, M. Steiner, U. Hiller, G.M. Kalvius, D.W. Mitchell, T.P. Das, P. Blaha, K. Schwarz, M.P. Pasternak, Phys. Rev. B 53 (1996) 11425.
[77] M. Valtiner, M. Todorova, G. Grundmeier, J. Neugebauer, Phys. Rev. Lett. 103 (2009) 065502.
[78] A. Gandubert, E. Krebs, C. Legens, D. Costa, D. Guillaume, P. Raybaud, Catal. Today 130 (2008) 149–159.
[79] J. Irrera Costa, Chem. Phys. 128 (2008) 114709.
[80] B. Diawara, L. Joubert, D. Costa, P. Marcus, C. Adamo, Surf. Sci. 603 (2009) 3025.
[81] D. Costa, P. Marcus, Surf. Sci. 604 (2010) 932.
[82] S. Chakarova-Kack, O. Borck, E. Schroder, B.I. Lundqvist, Phys. Rev. B 74 (2006) 155402.
[83] C. Wei, C. Tegenkamp, H. Pfnur, T.J. Bredow, Phys. Chem. C 114 (2010) 460.
[84] A. Tkatchenko, L. Romaner, O.T. Hofmann, E. Zojer, C. Ambrosch-Draxl, M. Scheffler, MRS Bull. 35 (2010) 435.
[85] S. Grimme, J. Antony, S. Ehrlich, H.J. Krieg, Chem. Phys. 132 (2010) 154104.
[86] C. Di Valentin, D. Costa, J. Phys. Chem. C, submitted for publication.
[87] F. Goltl, J. Hafner, J. Chem. Phys. 134 (2011) 064102.
[88] S. Tosoni, J. Sauer, Phys. Chem. Chem. Phys. 12 (2010) 14330.
[89] T. Becker, S. Hovel, M. Kunat, C. Boas, U. Burghaus, C. Wöll, Surf. Sci. 486 (2001) L502.
[90] F. Deproft, S. Amira, K. Choho, P. Geerlings, J. Phys. Chem. 98 (1994) 5227.
[91] S.V. Chong And, H. Idriss, Surf. Sci. 504 (2002) 145.
[92] C.M. Whelana, J. Ghijsen, J.-J. Pireaux, K. Maex, Thin Solid Films 464–465 (2004) 388.
[93] U. Gelius, P.F. Heden, J. Hedman, B.J. Lindberg, R. Manne, R. Nordberg, C. Nordling, K. Siegbahn, Phys. Scripta 2 (1970) 70.
[94] H. Idriss, P. Légare, G. Maire, Surf. Sci. 515 (2002) 413.
[95] R.A. Powell, W.E. Spicer, J.C. Mcmenamin, Phys. Rev. Lett. 27 (1971) 97.
[96] R.A. Powell, W.E. Spicer, J.C. Mcmenamin, Phys. Rev. B 6 (1972) 3056.
[97] R.T. Girard, O. Tjernberg, G. Chiaia, S. Söderholm, U.O. Karlsson, C. Wigren, H. Nylén, I. Lindau, Surf. Sci. 373 (1997) 409.
[98] T. Seto, T. Hara, K. Tanaka, Jpn. J. Appl. Phys. 7 (1968) 31.
[99] P. Fenter, P. Eisenberger, K.S. Liang, Phys. Rev. Lett. 70 (1993) 2447.
[100] D.J. Lavrich, S.M. Wetterer, S.L. Bernasek, G. Scoles, J. Phys. Chem. B 102 (1998) 3456.